Communications
doi.org/10.1002/batt.201900196

Chemistry Europe
European Chemical Societies Publishing

VIP *Very Important Paper*

Special Collection

Using a Heme-Based Nanozyme as Bifunctional Redox Mediator for Li–O_2 Batteries

Xiaowei Mu,[a] Yufeng Liu,[a] Xueping Zhang,[a] Hui Wei,[a] Ping He,*[a] and Haoshen Zhou*[a, b]

The realization of practical aprotic Li–O_2 batteries is hindered by superoxide-related parasitic reactions and high overpotentials. Herein, a heme-based nanozyme containing iron-porphyrin derivative ligands is used as a novel electrolyte additive to scavenge superoxide radicals in the Li–O_2 system. Specially, this type of nanozyme can act as a bifunctional catalyst for both discharge and charge by coordinating with superoxide intermediates, functioning as a molecular shuttle of superoxide species and electrons between cathodes and products. As a consequence, the Li–O_2 batteries exhibit boosted discharge capacity, reduced charge polarization and superior cycling stability in the presence of the nanozyme additive. This first attempt to using nanozyme in Li–O_2 batteries should pave a new way for the sustainable cross-link between biomimetic enzymes and advanced energy storage.

Rechargeable aprotic Li–O_2 batteries with ultra-high theoretical specific energy, ~3500 Wh kg^{-1}, have become the focus of scientific research and business application, which hold the promising potential in fields of electric vehicles and smart grids.[1] Typically, the operation of Li-O_2 batteries is based on the reversible formation and decomposition of Li_2O_2, following $2Li + O_2 \leftrightarrow Li_2O_2$, $E^0 = 2.96$ V vs. Li^+/Li.[2] During discharge, O_2 diffusing from cathode undergoes a one-electron reduction to form superoxide intermediates, which can be reduced electrochemically or disproportionate into Li_2O_2 (oxygen reduction reaction, ORR). These Li_2O_2 products are then oxidized to evolve O_2 upon charging (oxygen evolution reaction, OER). However, some fundamental challenges exist preventing the practical use of the state-of-the-art technology, especially the high overpotentials and severe side reactions.[3]

In fact, the two abovementioned challenges are closely correlated with each other, which are tightly related to the generation of superoxide intermediates and the inherent insulating and insoluble nature of Li_2O_2. Superoxide radical intermediates, as supernucleophiles, readily attack all cell components of organic electrolytes, binders and carbon-based cathodes.[4] The accumulation of byproducts during cycling blocks the multiphase reaction interface, giving rise to the serious ORR/OER polarization.[5] Besides, the oxidization of Li_2O_2 products with sluggish kinetics raises the charge potential inexorably, thus exacerbating parasitic reactions further.[6] Therefore, multitudes of efforts have been devoted to mitigate or solve these issues, including constructing stable and effective catalysts to reduce overpotentials,[7] adopting soluble additives into electrolytes to improve reaction dynamics[8] and developing new electrolytes resistive to reactive oxygen species, etc.[9]

Solid catalysts, like noble metals, transition metal oxides and nitrides, have been widely applied as cathode materials in Li-O_2 batteries, which certainly exhibit reduced polarization to different degree.[10] Nevertheless, the inherent large resistance resulted from the confined solid-solid contact between heterogeneous catalysts and products may inhibit efficient charge-transfer, thereby leading to relative limited catalytic activities. By contrast, soluble catalysts dissolved in electrolyte have been introduced as more fascinating candidates, which present superior performance owning to the sufficient contact area between liquid additives and solid products and their high utilization efficiency.[11] In particular, some electrolyte additives have been reported to serve as superoxide radical scavengers in Li-O_2 batteries, such as polydopamine,[12] cerium triflate,[13] hemoglobin[14] and so on.[15] As residual superoxide radicals are scavenged, the deposition of irreversible byproducts is alleviated and improved cycling stability is achieved. However, there is almost no promotion in specific capacity and discharge/charge voltage gap during deep-discharge operation in polydopamine or cerium triflate-involved systems.[12,13] Moreover, as for hemoglobin or heme, natural enzymes possess intrinsic limitations of poor stability, high cost and sensitivity to harsh environments.[14,16]

Nanomaterials with enzyme-like catalytic activities, known as nanozymes, can be used as stable and durable mimics to natural enzymes with highly catalytic activity.[17] Zhang's group has synthesized a series of archetypical metal-organic framework (MOF) nanosheets with intrinsic heme-like active sites to mimic peroxidases, which exhibit higher peroxide sensitivity compared with natural heme proteins.[18] Besides, Wei's group has pointed out that these MOF nanozymes can deliver enhanced peroxidase-mimicking activities than their bulk

[a] X. Mu, Y. Liu, X. Zhang, Prof. H. Wei, Prof. P. He, Prof. H. Zhou
Center of Energy Storage Materials & Technology,
College of Engineering and Applied Sciences,
Jiangsu Key Laboratory of Artificial Functional Materials,
National Laboratory of Solid State Microstructures and Collaborative Innovation Center of Advanced Microstructures
Nanjing University
Nanjing 210093, P.R. China
E-mail: pinghe@nju.edu.cn
hszhou@nju.edu.cn
[b] Prof. H. Zhou
Energy Technology Research Institute,
National Institute of Advanced Industrial Science and Technology (AIST)
Umezono 1-1-1, Tsukuba 3058568, Japan

Supporting information for this article is available on the WWW under https://doi.org/10.1002/batt.201900196

Special Collection *An invited contribution to a Special Collection on Electrolytes for Electrochemical Energy Storage*

analogues.[19] Furthermore, the heme-like ligands play a crucial role in determining the catalytic capability of nanozymes. As a proof-of-concept to investigate the radicals scavenging ability and catalytic activity of nanozymes with heme-like active centers, in this work, the MOF nanozyme composed of Fe(III) tetra(4-carboxyphenyl)porphine chloride (TCPP(Fe)) ligands and Zn metal nodes (denoted as Zn-TCPP(Fe)) is applied as a novel electrolyte additive in the Li–O_2 system. It is found that the Zn-TCPP(Fe) nanozymes can perform as the bifunctional catalyst for both discharge and recharge processes by coordinating with superoxide intermediates, functioning as a molecular shuttle of superoxide species and electrons between cathodes and products. As a result, the Li-O_2 batteries show enlarged discharge capacity, enhanced energy efficiency and superior cycling stability with the addition of Zn-TCPP(Fe) nanozymes.

Herein, the Zn-TCPP(Fe) MOF nanozyme was synthesized by using a surfactant-assisted method (see the Experimental Section in the Supporting Information for details),[18,19] as illustrated in Figure 1a. According to previous studies, the heme-like TCPP(Fe) ligands serve as catalytic active sites, metal nodes act as structural building blocks, and the polyvinylpyrrolidone (PVP) is employed as surfactant to control the growth of MOF crystals. During the reaction, one TCPP(Fe) ligand is interconnected by four $Zn_2(COO)_4$ paddlewheel metal nodes to form a 2D layered nanosheet. X-ray diffraction (XRD) and transmission electron microscopy (TEM) were taken to characterize the crystal structure and morphology of Zn-TCPP(Fe) nanosheets. As shown in Figure S1a, three peaks at 7.6°, 8.8°, and 17° can been seen, which is consistent with that has been reported.[18,19] And the TEM image in Figure S1b clearly reveals the 2D Zn-TCPP(Fe) MOF with well-defined ultrathin sheet-like structures.

The superoxide radical scavenging capability or the oxygen binding ability of Zn-TCPP(Fe) nanozymes was evaluated via the nitro-blue tetrazolium (NBT) reduction test and characterized by UV-visible spectroscopy (UV-vis).[12,13,15] KO_2 and crown ether were added into 1.0 M lithium bis(trifluoromethanesulphonyl)imide/tetraethylene glycol dimethyl ether (LiTFSI/TEGDME) electrolyte to generate superoxide radicals. The TEGDME-based electrolyte was used due to its relatively high chemical stability and low volatility.[20] Because of the linear relationship between the superoxide radical concentration and the UV-vis absorbance intensity centered at 560 nm of the NBT solution (Figure S2), the superoxide radical concentration can be quantified. It can be seen from Figure 1b that the introduction of Zn-TCPP(Fe) nanozymes into NBT solutions results in the color change from blue to faint yellow and the disappearance of characteristic UV-vis absorption peaks, demonstrating the dramatic radical scavenging capability of Zn-TCPP(Fe) nanozymes. Moreover, the UV-vis absorbance intensity decreases with the increase of Zn-TCPP(Fe) concentration. As the Zn-TCPP(Fe) concentration increases from 0.5 mM to 2 mM, the residual superoxide radical concentration is reduced from 13.10% to 2.49% (Figure 1c).

Cyclic voltammetry (CV) measurements conducted on an Au electrode were carried out to investigate the catalytic function of Zn-TCPP(Fe) nanozymes in a typical Li–O_2 cell (Figure 2). One cathodic peak at 2.57 V ($E_{c,1}$) and one anodic peak at 3.26 V ($E_{a,1}$) appear in the cell without Zn-TCPP(Fe) under O_2 atmosphere, corresponding to the formation and decomposition of Li_2O_2 products, respectively.[16] With the addition of Zn-TCPP(Fe), the cell operated in Ar displays a cathodic peak at 2.25 V ($E_{c,3}$) and an anodic peak at 3.62 V ($E_{a,2}$), which are ascribed to the electron transfer of Fe active centers in Zn-TCPP(Fe), depicted as $Fe^{3+} + e^- \rightarrow Fe^{2+}$ and $Fe^{2+} - e^- \rightarrow Fe^{3+}$, respectively. Upon O_2 purging, a broad cathodic peak located at 2.48 V ($E_{c,2}$) with similar onset potential with the bare Li-O_2 cell emerges, which is attributed to the promoted ORR by the adduct $(Zn-TCPP(Fe))-O_2^-$.[21] Meanwhile, a new anodic peak at 3.70 V ($E_{a,3}$) following the oxidation of Fe active centers arises. It is reasonable to ascribe this peak to the oxidation of $(Zn-TCPP(Fe))-O_2^-$. Thus, the Zn-TCPP(Fe)

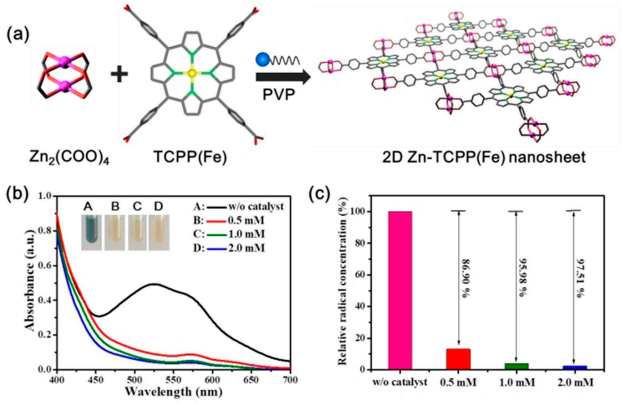

Figure 1. (a) Schematic illustration of the surfactant-assisted synthesis of 2D Zn-TCPP(Fe) nanosheet. (b) UV-vis spectra of NBT solutions at different Zn-TCPP(Fe) concentrations. Inset: corresponding photograph images of NBT solutions in test tubes. (c) The remaining radical concentration as a function of the Zn-TCPP(Fe) concentration.

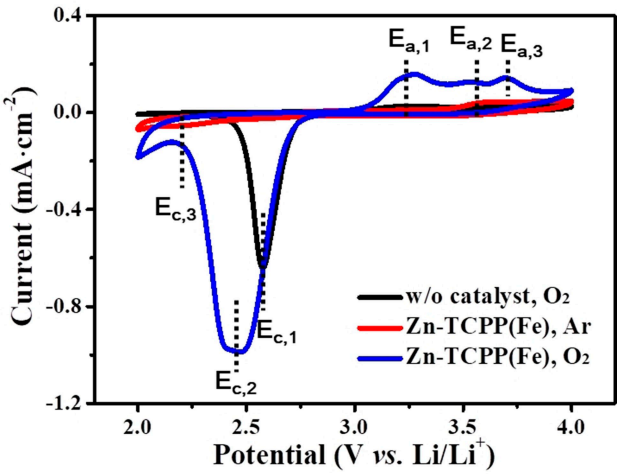

Figure 2. CV curves obtained on an Au electrode in 1.0 M LiTFSI/TEGDME containing 1.0 mM Zn-TCPP(Fe) under Ar (red curve) and O_2 (blue curves). For comparison, the CV curve in the absence of Zn-TCPP(Fe) is also included (black curve). The scan rate is 20 mV s^{-1}.

nanozyme is expected to perform as an ORR/OER bifunctional catalyst in Li-O_2 batteries.

To assess the practical electrochemical performance of Zn-TCPP(Fe) in Li–O_2 batteries, galvanostatic discharge-charge tests of batteries using Super P (SP) carbon cathodes with and without Zn-TCPP(Fe) under O_2 were conducted. As shown in Figure 3a and 3b, both of the batteries with Zn-TCPP(Fe) deliver reduced overpotentials about 270 mV than those in the absence of Zn-TCPP(Fe) under the same conditions. A specific discharge capacity of 6750 mAh g^{-1} is obtained at the current density of 100 mA g^{-1} with the addition of Zn-TCPP(Fe) during deep-discharge operation, more than twice as much as that without Zn-TCPP(Fe). Even at higher current densities of 200 and 400 mA g^{-1}, discharge capacities of 6220 and 5230 mAh g^{-1} can be achieved (Figure 3c), revealing the excellent rate capability of Zn-TCPP(Fe)-involved Li–O_2 batteries. In contrast, the Li–O_2 battery containing Zn-TCPP exhibits lower specific capacity of 3840 mAh g^{-1} and larger charge polarization (Figure S3), declaring the electrocatalytic active sites of Fe centers in Zn-TCPP(Fe). CV results are combined to explain the improved electrochemical performance of batteries in the presence of Zn-TCPP(Fe) nanozymes. In the discharge process, O_2 is reduced into superoxide intermediates primarily. Most of superoxide intermediates can be captured by Fe active centers of Zn-TCPP(Fe), forming $(Zn-TCPP(Fe))-O_2^-$ in electrolyte. The $(Zn-TCPP(Fe))-O_2^-$ binds with Li^+ and is reduced on the cathode or disproportionated to generate Li_2O_2 products and Zn-TCPP(Fe) via the solution-phase reaction route, which will

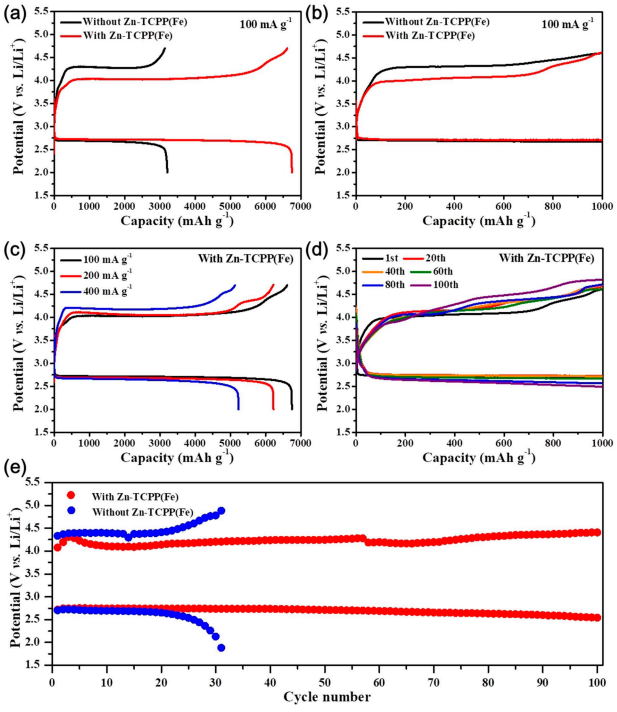

Figure 3. Galvanostatic discharge-charge tests of Li–O_2 batteries with and without Zn-TCPP(Fe) during deep-discharge operation (a) and under fixed specific capacities of 1000 mAh g^{-1} (b). (c) Rate capability and (d) cycle performance of Li–O_2 batteries with Zn-TCPP(Fe). (e) The discharge and charge plateau potentials at different cycles.

be supported by the morphology of products afterwards.[11b,22] Benefiting from the solution-mediated growth of Li_2O_2, the discharge capacity is promoted greatly. In the subsequent charging process, Li_2O_2 is oxidized to form superoxide intermediates, which are combined with Zn-TCPP(Fe) into $(Zn-TCPP(Fe))-O_2^-$ continually. The direct decomposition of Li_2O_2 is then converted into the oxidation of $(Zn-TCPP(Fe))-O_2^-$ tactfully, facilitating to the lowered charge polarization.[11a,c] Notably, the Fe^{3+}/Fe^{2+} redox couple of Fe active centers does not participant in the discharge-charge process actually, whose potential is situated in the range of sudden death. Without the participant of O_2, negligible capacity is shown in the Zn-TCPP(Fe)-involved battery (Figure S4).

One the one hand, the aggressive superoxide radicals are scavenged by Zn-TCPP(Fe) nanozymes efficiently,[12–15] which is beneficial for the enhanced stability of electrolyte and cathode during the battery operation. On the other hand, the Zn-TCPP (Fe) nanozymes can act as superoxide and electron carriers between the cathode and Li_2O_2, serving as effective ORR/OER redox mediators in Li-O_2 batteries.[11c,16] These advantages enable the Zn-TCPP(Fe)-containing Li-O_2 battery a superior cycling performance. Under the fixed specific capacity of 1000 mAh g^{-1} at a current density of 100 mA g^{-1}, the Li-O_2 battery with the addition of Zn-TCPP(Fe) exhibits steady discharge-charge behavior (Figure 3d). In contrast to the stable cycling over 100 cycles with Zn-TCPP(Fe), the battery without Zn-TCPP(Fe) can only run about 30 cycles (Figure 3e). The gradual enlarged voltage hysteresis is supposed to be caused by the accumulation of irreversible parasitic byproducts, such as Li_2CO_3 and LiCOOR.[3c,4e,5a]

The morphology and composition of SP cathodes in Li-O_2 batteries with Zn-TCPP(Fe) nanozymes during different reaction stages were characterized by scanning electron microscopy (SEM), XRD, Raman and X-ray photoelectron spectroscopy (XPS). Figure S5a shows the typical morphology of SP carbon particles. After discharge, large-size toroids with diameters of 2–3 μm are deposited on the surface of SP cathode (Figure 4a), supporting the solution-mediated growth of Li_2O_2 as stated before.[11b,22] When the recharge process is finished, those toroidal particles disappear and the cathode surface is recovered (Figure 4b). Moreover, it can be seen in Figure 4c that the obtained new diffraction peaks after discharge are indexed to sole Li_2O_2 (PDF#09-0355), which is decomposed totally after recharge. No other peaks of products but Li_2O_2 (786 cm^{-1}) are observed in the Raman spectra (Figure 4d), in good coincide with results of XRD analysis. Furthermore, compared to the pristine cathode before electrochemical test (Figure S5b), the deconvoluted C 1s spectrum of the bare battery after discharge in Figure 4e shows three grown peaks at 286.3, 287 and 289.8 eV, which are assigned to ether/alkoxides, carboxylates, and carbonates of parasitic products, respectively.[12] Remarkably, the Zn-TCPP(Fe)-incorporated battery exhibits distinct smaller peaks (Figure 4e), verifying the significantly suppressed side reactions owning to the efficient scavenging of reactive superoxide radicals. A small amount of Li_2CO_3 arises, which might be caused by the transient exposure to air during sampling process. No peak of Li_2CO_3 or Li_2O_2 is observed after

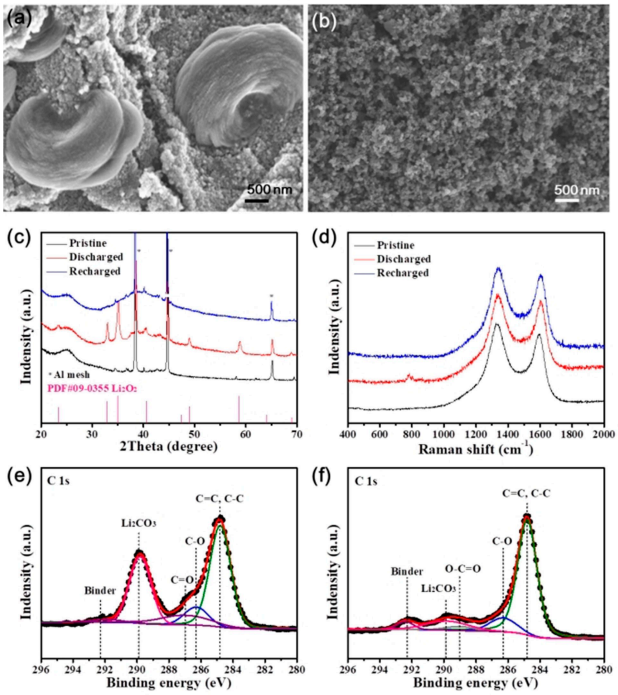

Figure 4. SEM images of SP cathodes during different reaction stages in Li-O_2 batteries with Zn-TCPP(Fe): (a) after discharge and (b) after recharge. (c) XRD patterns and (d) Raman spectra of SP cathodes during different reaction stages with Zn-TCPP(Fe). XPS spectra of discharged SP cathodes (e) without Zn-TCPP(Fe) and (f) with Zn-TCPP(Fe).

recharge (Figure S6), confirming the improved reversibility of Li-O_2 batteries with the introduction of Zn-TCPP(Fe) nanozymes. Even though there is a tendency of moderately growing signals for carbonates and carboxylates in the battery with Zn-TCPP (Fe), the accumulation of these side products is much more severe without Zn-TCPP(Fe) after cycling (Figure S7).

Some natural enzymes, like coenzyme Q_{10}[22] and vitamin K2[11d] have been reported to be applied as soluble additives in Li-O_2 batteries. Serving as ORR redox mediators, the discharge capacities and rate capabilities of batteries are boosted remarkably. However, all these batteries show poor rechargeability due to the solution-mediated growth of large-size Li_2O_2.[23] Heme molecules have been adopted by Taylor's group in 2016, which can take effect both in discharge and charge processes because of the redox couple of Fe^{3+}/Fe^{2+}.[16] Subsequently, Bhattacharyya et al. have revealed that heme is not a suitable redox mediator with lesser stability during cycling in Li–O_2 batteries.[14] In particular, the Zn-TCPP(Fe) nanozymes composed of heme-like ligands, possess characteristics of highly catalytic activity and superior robustness.[19] The specific reaction mechanism of Li–O_2 batteries with Zn-TCPP (Fe) nanozymes can be summarized in Equations (1)–(7):

During discharge:

$$O_2+e^-\rightarrow O_2^- \quad (1)$$

$$Zn-TCPP(Fe)+O_2^-\rightarrow(Zn-TCPP(Fe))-O_2^- \quad (2)$$

$$2(Zn-TCPP(Fe))-O_2^-+2Li^+\rightarrow 2Zn-TCPP(Fe)+Li_2O_2+O_2 \quad (3)$$

$$(Zn-TCPP(Fe))-O_2^-+2Li^++e^-\rightarrow Zn-TCPP(Fe)+Li_2O_2 \quad (4)$$

During recharge:

$$Li_2O_2-e^-\rightarrow 2Li^++O_2^- \quad (5)$$

$$Zn-TCPP(Fe)+O_2^-\rightarrow(Zn-TCPP(Fe))-O_2^- \quad (6)$$

$$(Zn-TCPP(Fe))-O_2^--e^-\rightarrow Zn-TCPP(Fe)+O_2 \quad (7)$$

Interestingly, the new mechanism involving $(Zn-TCPP(Fe))-O_2^-$ intermediates suppresses the superoxide-related side reactions effectively. Moreover, the Zn-TCPP(Fe) nanozyme is applied as an ORR/OER bifunctional redox mediators, acting as a molecular shuttle of superoxide species and electrons between cathodes and products.[24] What's more, the MOF nanozymes are promising biomimetic catalysts with multiple catalytic active sites, tailorable structures, high robustness and convenient recyclability.[19] Our first attempt to using nanozymes in Li–O_2 batteries should pave a new way for the sustainable cross-link between biomimetic enzymes and advanced energy storage.

In conclusion, the heme-based Zn-TCPP(Fe) MOF nanozymes are used as the bifunctional redox mediators in Li–O_2 batteries. On the one hand, the aggressive superoxide intermediates are scavenged efficiently by Zn-TCPP(Fe). On the other hand, Zn-TCPP(Fe) can perform as a molecular shuttle of superoxide species and electrons between cathodes and products by combing with superoxides. These unique features guarantee the Zn-TCPP(Fe)-involved Li–O_2 batteries a boosted discharge capacity, enhanced energy efficiency and superior cycling performance. Moreover, this is the first attempt to using nanozyme in Li–O_2 batteries, which should pave a new way for the sustainable cross-link between biomimetic enzymes and advanced energy storage.

Acknowledgements

This research was partially supported by the National Key Research and Development Program of China (2016YFB0100203), National Natural Science Foundation of China (21922508, 21673116, 21633003, U1801251), Natural Science Foundation of Jiangsu Province of China (BK20190009) and PAPD of Jiangsu Higher Education Institutions.

Keywords: nanozyme · superoxide radical scavenging · bifunctional redox mediator · Li–O_2 battery · cycling stability

[1] a) D. Andre, H. Hain, P. Lamp, F. Maglia, B. Stiaszny, *J. Mater. Chem. A* **2017**, *5*, 17174–17198; b) J. W. Choi, D. Aurbach, *Nat. Rev. Mater.* **2016**, *1*, 16013; c) P. G. Bruce, S. A. Freunberger, L. J. Hardwick, J. M. Tarascon, *Nat. Mater.* **2012**, *11*, 19–29.

[2] a) N. Imanishi, A. C. Luntz, P. Bruce, *The lithium air battery: fundamentals*, Springer, New York, **2014**; b) J. Lu, L. Li, J. B. Park, Y. K. Sun, F. Wu, K. Amine, *Chem. Rev.* **2014**, *114*, 5611–5640; c) H. D. Lim, B. Lee, Y. Bae, H. Park, Y. Ko, H. Kim, J. Kim, K. Kang, *Chem. Soc. Rev.* **2017**, *46*, 2873–2888.
[3] a) A. C. Luntz, B. D. McCloskey, *Chem. Rev.* **2014**, *114*, 11721–11750; b) A. Eftekhari, *Sustain. Energ. Fuels* **2017**, *1*, 2053–2060; c) Y. Liu, L. Wang, L. Cao, C. Shang, Z. Wang, H. Wang, L. He, J. Yang, H. Cheng, J. Li, Z. Lu, *Mater. Chem. Front.* **2017**, *1*, 2495–2510; d) F. Li, T. Zhang, H. Zhou, *Energy Environ. Sci.* **2013**, *6*, 1125–1141; e) D. Geng, D. Ning, T. S. A. Hor, S. W. Chien, Z. Liu, D. Wuu, X. Sun, Y. Zong, *Adv. Energy Mater.* **2016**, *6, 1502164*.
[4] a) S. A. Freunberger, Y. Chen, N. E. Drewett, L. J. Hardwick, F. Bardé, P. G. Bruce, *Angew. Chem. Int. Ed.* **2011**, *50*, 8609–8613; *Angew. Chem.* **2011**, *123*, 8768–8772; b) D. G. Kwabi, T. P. Batcho, C. V. Amanchukwu, N. Ortiz-Vitoriano, P. Hammond, C. V. Thompson, Y. Shao-Horn, *J. Phys. Chem. Lett.* **2014**, *5*, 2850–2856; c) R. Black, H. O. Si, J. H. Lee, T. Yim, B. Adams, L. F. Nazar, *J. Am. Chem. Soc.* **2012**, *134*, 2902–2905; d) K. R. Ryan, L. Trahey, B. J. Ingram, A. K. Burrell, *J. Phys. Chem. C* **2012**, *116*, 19724–19728; e) M. M. O. Thotiyl, S. A. Freunberger, Z. Peng, P. G. Bruce, *J. Am. Chem. Soc.* **2012**, *135*, 494–500.
[5] a) B. M. Gallant, R. R. Mitchell, D. G. Kwabi, J. Zhou, L. Zuin, C. V. Thompson, Y. Shao-Horn, *J. Phys. Chem. C* **2012**, *116*, 20800–20805; b) B. D. Mccloskey, A. Speidel, R. Scheffler, D. C. Miller, V. Viswanathan, J. S. Hummelshøj, J. K. Nørskov, A. C. Luntz, *J. Phys. Chem. Lett.* **2012**, *3*, 997–1001.
[6] a) V. Viswanathan, K. S. Thygesen, J. S. Hummelshøj, J. K. Nørskov1, G. Girishkumar, B. D. McCloskey, A. C. Luntz, *J. Chem. Phys.* **2011**, *135*, 214704; b) S. Ganapathy, B. D. Adams, G. Stenou, M. S. Anastasaki, K. Goubitz, X. F. Miao, L. F. Nazar, M. Wagemaker, *J. Am. Chem. Soc.* **2014**, *136*, 16335–16344.
[7] a) H. O. Si, L. F. Nazar, *Adv. Energy Mater.* **2012**, *2*, 903–910; b) Y. Bae, H. Park, Y. Ko, H. Kim, S. K. Park, K. Kang, *Batteries & Supercaps* **2019**, *2*, 311–325; Supercaps **2019**, 2, 311–325; c) M. Balaish, J. W. Jung, I. D. Kim, Y. Ein-Eli, *Adv. Funct. Mater.* **2019**, 10.1002/adfm.201808303.
[8] a) Y. Chen, X. Gao, L. R. Johnson, P. G. Bruce, *Nat. Commun.* **2018**, *9*, *767*; b) J. B. Park, S. H. Lee, H. G. Jung, D. Aurbach, Y. K. Sun, *Adv. Mater.* **2018**, *30, 1704162*; c) Y. Ko, H. Park, B. Kim, J. S. Kim, K. Kang, *Trends in Chemistry* **2019**, *1*, 349–360.
[9] a) J. Lai, Y. Xing, N. Chen, L. Li, F. Wu, R. Chen, *Angew. Chem. Int. Ed.* **2019**, 10.1002/anie.201903459; b) Z. Liu, J. Huang, Y. Zhang, B. Tong, F. Guo, J. Wang, Y. Shi, R. Wen, Z. Zhou, L. Guo, Z. Peng, *Adv. Energy Mater.* **2019**, *9*, 1901967; c) Y. Xing, N. Chen, M. Luo, Y. Sun, Y. Yang, J. Qian, L. Li, S. Guo, R. Chen, F. Wu, *Energy Storage Mater.* **2019**, 10.1016/j.ensm.2019.06.008; d) J. Zhang, B. Sun, Y. Zhao, A. Tkacheva, Z. Liu, K. Yan, X. Guo, A. M. McDonagh, D. Shanmukaraj, C. Wang, T. Rojo, M. Armand, Z. Peng, G. Wang, *Nat. Commun.* **2019**, *10*, 602; e) W. Zhang, Y. Huang, Y. Liu, L. Wang, S. Chou, H. Liu, *Adv. Energy Mater.* **2019**, *9*, 1900464.
[10] a) B. D. Mccloskey, R. Scheffler, A. Speidel, D. S. Bethune, R. M. Shelby, A. C. Luntz, *J. Am. Chem. Soc.* **2011**, *133*, 18038–18041; b) Z. Peng, S. A. Freunberger, Y. Chen, P. G. Bruce, *Science* **2012**, *337*, 563–566; c) Z. Jian, P. Liu, F. Li, P. He, X. Guo, M. Chen, H. Zhou, *Angew. Chem. Int. Ed.* **2014**, *53*, 442–446; *Angew. Chem.* **2014**, *126*, 452–456; d) W. Yao, Y. Yuan, G. Tan, C. Liu, M. Cheng, V. Yurkiv, X. Bi, F. Long, C. R. Friedrich, F. Mashayek, K. Amine, J. Lu, R. Shahbazian-Yassar, *J. Am. Chem. Soc.* **2019**, *141*, 12832–12838.
[11] a) Y. Chen, S. A. Freunberger, Z. Peng, O. Fontaine, P. G. Bruce, *Nat. Chem.* **2013**, *5*, 489–494; b) X. Gao, Y. Chen, L. Johnson, P. G. Bruce, *Nat. Mater.* **2016**, *15*, 882–888; c) D. Sun, Y. Shen, W. Zhang, L. Yu, Z. Yi, W. Yin, D. Wang, Y. Huang, J. Wang, D. Wang, J. B. Goodenough, *J. Am. Chem. Soc.* **2014**, *136*, 8941–8946; d) Y. Ko, H. Park, J. Kim, H. D. Lim, B. Lee, G. Kwon, S. Lee, Y. Bae, S. K. Park, K. Kang, *Adv. Funct. Mater.* **2019**, *29*, 1805623.
[12] B. G. Kim, S. Kim, H. Lee, J. W. Choi, *Chem. Mater.* 2014, 26, 4757–4764.
[13] Z. Wang, S. Tian, B. Shao, S. Li, L. Li, J. Yang, *J. Power Sources* **2019**, *414*, 327–332.
[14] R. N. Samajdar, S. M. George, A. J. Bhattacharyya, *J. Phys. Chem. C* **2019**, *123*, 23433–23438.
[15] a) S. E. Jerng, T. Y. Kim, S. Bae, J. Shin, J. Park, J. Yi, J. W. Choi, *Energy Storage Mater.* **2019**, *19*, 16–23; b) C. Wu, T. Li, C. Liao, L. Li, J. Yang, *J. Mater. Chem. A* **2019**, *5*, 12782–12786.
[16] W. H. Ryu, F. S. Gittleson, J. M. Thomsen, J. Li, M. J. Schwab, G. W. Brudvig, A. D. Taylor, *Nat. Commun.* **2016**, *7*, 12925.
[17] H. Wei, E. Wang, *Chem. Soc. Rev.* **2013**, *42*, 6060.
[18] a) Y. Wang, M. Zhao, J. Ping, B. Chen, X. Cao, Y. Huang, C. Tan, Q. Ma, S. Wu, Y. Yu, Q. Lu, J. Chen, W. Zhao, Y. Ying, H. Zhang, *Adv. Mater.* **2016**, *28*, 4149–4155; b) M. Zhao, Y. Wang, Q. Ma, Y. Huang, X. Zhang, J. Ping, Z. Zhang, Q. Lu, Y. Yu, H. Xu, Y. Zhao, H. Zhang, *Adv. Mater.* **2015**, *27*, 7372–7378.
[19] H. Cheng, Y. Liu, Y. Hu, Y. Ding, S. Lin, W. Cao, Q. Wang, J. Wu, F. Muhammad, X. Zhao, D. Zhao, Z. Li, H. Xing, H. Wei, *Anal. Chem.* **2017**, *89,* 11552–11559.
[20] M. Tang, J. C. Chang, S. R. Kumar, S. J. Lue, *Energy* **2019**, *187*, 115926.
[21] X. Hu, J. Wang, Z. Li, J. Wang, D. H. Gregory, J. Chen, *Nano Lett.* **2017**, *17*, 2073–2078.
[22] Y. Zhang, L. Wang, X. Zhang, L. Guo, Y. Wang, Z. Peng, *Adv. Mater.* **2017**, *30*, 1705571.
[23] L. Wang, Y. Zhang, Z. Liu, L. Guo, Z. Peng, *Green Energy Environ.* **2017**, *2*, 186–203.
[24] X. Wang, Z. Zhang, Q. Zhang, C. Wang, X. Zhang, Z. Xie, Z. Zhou, *J. Mater. Chem. A* **2019**, *7*, 14239–14243.

Manuscript received: November 30, 2019
Revised manuscript received: January 2, 2020
Accepted manuscript online: January 10, 2020
Version of record online: January 22, 2020